






## Mutual friction and diffusion of two-dimensional quantum vortices

Zain Mehdi <sup>1,\*</sup> Joseph J. Hope <sup>1</sup> Stuart S. Szigeti <sup>1</sup> and Ashton S. Bradley <sup>2</sup>

<sup>1</sup>*Department of Quantum Science and Technology and Department of Fundamental and Theoretical Physics, Research School of Physics, Australian National University, Canberra 2600, Australia*

<sup>2</sup>*Dodd-Walls Centre for Photonic and Quantum Technologies, Department of Physics, University of Otago, Dunedin 9016, Aotearoa New Zealand*

 (Received 9 May 2022; revised 23 September 2022; accepted 2 March 2023; published 16 March 2023)

Dissipation of quantum vortex motion is fundamental to superfluid dynamics and quantum turbulence, yet there is currently a large gap between theory and experiments with ultracold atoms. Here we present a microscopic open quantum systems theory of thermally damped vortex motion in oblate atomic superfluids that includes previously neglected energy-damping interactions between superfluid and thermal atoms. This mechanism couples strongly to vortex core motion and causes dissipation of vortex energy due to mutual friction, as well as Brownian motion of vortices due to thermal fluctuations. We derive an analytic expression for the dimensionless mutual friction coefficient that gives excellent quantitative agreement with experimentally measured values, without any fitted parameters. Our work closes an existing two orders of magnitude gap between dissipation theory and experiments, previously bridged by fitted parameters, and provides a microscopic origin for the mutual friction and diffusion of quantized vortices in two-dimensional atomic superfluids.

DOI: [10.1103/PhysRevResearch.5.013184](https://doi.org/10.1103/PhysRevResearch.5.013184)

### I. INTRODUCTION

Quantum vortex dynamics are central to many superfluid phenomena, including the Kibble-Zurek mechanism [1], Berezinskii-Kosterlitz-Thouless (BKT) transition [2,3], persistent current decay [4,5], and type II superconductivity [6]. Planar atomic superfluids offer an ideal platform for studying nonequilibrium superfluid behavior, with dynamics significantly simplified by forcing vortex lines to align with the tightly confined axis and move as points in the plane [7] in perfect analogy to two-dimensional (2D) electrodynamics [8]. Experimentally, these systems have demonstrated powerful capabilities for studying incompressible “point-vortex” turbulence [9–12], arguably the simplest manifestation of 2D turbulent flow [13].

Dissipation of vortex energy is an important aspect of the nonequilibrium dynamics of 2D quantum vortices, and is critical to spectral energy transport [14], turbulent cascades [15], the emergence of negative-temperature vortex clusters [9,16,17], and turbulent relaxation of vortex matter [11,12,18]. In superfluid helium, vortex dissipation is understood as arising due to “mutual friction” between moving vortices and the normal component of the fluid [19–21]. This approach reduces to phenomenology for weakly interacting systems which cannot be described within a two-fluid approximation, leaving the microscopic origin of thermal dissipation

of vortex energy in atomic superfluids an important open question.

Although the conservative dynamics of point vortices in 2D superfluids are well described by the Helmholtz-Kirchoff point-vortex model (PVM) [22,23], there is currently no microscopic theory of 2D vortex dynamics that can *ab initio* account for vortex dissipation observed in experiment. Existing microscopic estimates of vortex damping rates [24,25] are orders of magnitude lower than observed in experiments [9,11,12,17,26,27], requiring vortex damping to be treated phenomenologically as a fitted parameter [9–12,17,26]. Furthermore, there exists no microscopic theory for recent observations of vortex diffusion driven by Brownian motion [12]. The lack of a complete theory of vortex damping and noise is therefore a significant barrier to establishing a strong understanding of 2D vortex dynamics and superfluid turbulence.

In this work, we present a microscopic model of quantum vortex damping and diffusion in 2D due to thermal friction, derived from first-principles reservoir theory of finite-temperature atomic Bose gases. Our approach identifies the number-conserving scattering between superfluid and thermal atoms as the dominant vortex dissipation mechanism, contrasting with previous approaches that neglect this interaction and focus instead on Bose-enhanced particle transfer between superfluid and normal fluid. Our model includes both a dissipative mutual friction term and a stochastic term that describes the Brownian motion of vortices due to thermal fluctuations; crucially, it contains no fitted parameters and allows the mutual friction coefficient to be determined analytically from first principles. Our microscopic model’s predictions are in close quantitative agreement with previous experimental measurements of the mutual friction coefficient. This establishes a microscopic justification for vortex damping phenomenology

\*zain.mehdi@anu.edu.au

Published by the American Physical Society under the terms of the [Creative Commons Attribution 4.0 International license](https://creativecommons.org/licenses/by/4.0/). Further distribution of this work must maintain attribution to the author(s) and the published article’s title, journal citation, and DOI.

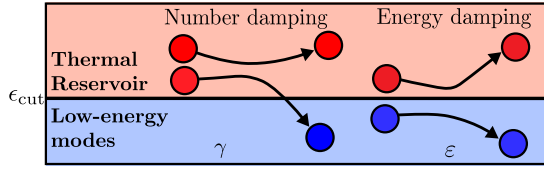


FIG. 1. The two reservoir processes described by SPGPE theory. Number damping ( $\gamma$ ) involves interatomic scattering that transfers atoms from the high occupation low-energy modes to the thermal reservoir and vice versa, e.g., a collision of two reservoir atoms that transfers most of the collision energy to one atom, leaving the other in a low-energy mode. Energy damping ( $\epsilon$ ), in contrast, describes number-conserving scattering interactions that exchange energy between the low-energy modes and reservoir without exchanging atoms.

and opens the door for quantitative *ab initio* modeling of two-dimensional quantum turbulence (2DQT) experiments using stochastic point vortex theory.

## II. VORTEX DISSIPATION PHENOMENOLOGY

The dynamics of dissipative 2D point vortices in atomic superfluids is accurately described by the PVM with the addition of a phenomenological longitudinal damping force [9,11,12,17,26,27]. For a system of  $N$  point vortices with positions  $\mathbf{r}_i(t) = (X_i(t), Y_i(t), 0)$  and unit charges  $\hbar q_i/m = \pm \hbar/m$ , this gives the “damped-PVM”:

$$\dot{\mathbf{r}}_i = \mathbf{v}_i^0 - \alpha q_i \hat{\mathbf{z}} \times \mathbf{v}_i^0. \quad (1)$$

Here  $\mathbf{v}_i^0 = \frac{\hbar}{m} \sum_{j \neq i} \frac{q_j}{r_{ij}^2} (Y_j - Y_i, X_i - X_j, 0)$  is the local superfluid velocity at the  $i$ th vortex, with  $r_{ij}^2 \equiv (X_i - X_j)^2 + (Y_i - Y_j)^2$ ,  $\hat{\mathbf{z}}$  is the unit vector perpendicular to the 2D superfluid plane, and  $\alpha$  is the dimensionless mutual friction coefficient. Note  $\alpha = 0$  gives the idealized PVM. The damped-PVM can be derived from a variational treatment of the dissipative GPE (dGPE) [28], a complex Ginzburg-Landau equation where an imaginary component is added to the prefactor of the GPE.

Dissipation of this type can be microscopically justified based on reservoir interactions between the partially coherent modes of the quantum field and the sparsely occupied high-energy incoherent modes which act as a thermal bath. This can be described by the stochastic projected GPE (SPGPE), a first-principles reservoir theory that formally divides the reservoir modes from the low-energy modes by an energy cutoff  $\epsilon_{\text{cut}}$  (a brief review of SPGPE theory is provided in Appendix A). Specifically, damping of this form arises due to *number damping* reservoir interactions where interatomic scattering transfers atoms from the superfluid to the thermal reservoir (or vice versa); see Fig. 1. Based on this process, the mutual friction coefficient  $\alpha$  in Eq. (1) corresponds to the first-principles dimensionless parameter  $\gamma \sim 8a_s^2/\lambda_{\text{th}}^2$  [28], where  $a_s$  the s-wave scattering length and  $\lambda_{\text{th}}$  is the thermal de Broglie wavelength. Typically,  $\gamma$  is of order  $10^{-5}$  [29], orders of magnitude too weak to account for the mutual friction coefficients  $\alpha \sim 10^{-2}$  observed in experiment [26]. Additionally, the damped-PVM does not include the effect incoherent thermal fluctuations described by SPGPE theory, limiting its

validity to relatively low temperatures far from the critical temperature.

In addition to number damping, SPGPE theory also contains a second reservoir process in which energy is exchanged due to number-conserving scattering interactions between superfluid and thermal atoms (Fig. 1). This process, called *energy damping*, has been neglected in almost all SPGPE studies to date, often under the justification that it is expected to be weak near equilibrium [24,25]. Only a handful of recent theoretical investigations have included energy damping, following developments in numerical techniques that have enabled simulation of the full SPGPE [30–34]. Notably, Ref. [31] studied the effect of both reservoir processes on the dissipation of a single vortex in a harmonically trapped three-dimensional (3D) gas, finding that energy damping was the dominant process in the regime studied. This is consistent with the results presented here, where we find that the energy-damping process is the dominant mechanism of point-vortex damping by two orders of magnitude.

## III. MICROSCOPIC THEORY OF FINITE-TEMPERATURE POINT VORTICES

Our model of finite-temperature point-vortex dynamics is constructed within the framework of SPGPE theory, explicitly including the energy-damping terms and neglecting the number-damping process, precisely the opposite approach taken in previous work. Our starting point is the quasi-2D SPGPE (Appendix B), neglecting number-damping terms [35]:

$$i\hbar d\psi = (\mathcal{L} - \mu)\psi dt + (V_\epsilon dt - \hbar dU_\epsilon)\psi, \quad (2)$$

where  $\psi(\mathbf{x}, t)$  is a classical field describing the finite-temperature superfluid dynamics in the plane  $\mathbf{x} = (x, y)$ ,  $\mathcal{L} = (-\hbar^2 \nabla^2 / (2m) + g|\psi|^2)\psi$  is the Gross-Pitaevskii (GP) operator,  $\mu$  is the chemical potential, and spatial and temporal arguments are suppressed for brevity.  $i\hbar d\psi = (\mathcal{L} - \mu)\psi dt$  is precisely the GPE describing the conservative dynamics of the highly occupied modes that host the vortices, and remaining are reservoir terms. The energy-damping reservoir process leads to dissipation described by an effective scattering potential [36]

$$V_\epsilon(\mathbf{x}) = \hbar \int d^2 \mathbf{x}' \epsilon(\mathbf{x} - \mathbf{x}') \frac{d\rho(\mathbf{x}')}{dt} \quad (3)$$

that damps changes in the fluid density  $\rho = |\psi|^2$ . Here  $\epsilon(\mathbf{x})$  is the 2D scattering kernel. Associated with energy-damping dissipation is a Gaussian noise term representing incoherent thermal fluctuations, satisfying correlations  $\langle dU_\epsilon \rangle = 0$  and  $\hbar \langle dU_\epsilon(\mathbf{x}, t) dU_\epsilon(\mathbf{x}', t') \rangle = 2k_B T \epsilon(\mathbf{x} - \mathbf{x}') \delta(t - t') dt$ . Both the scattering potential and noise correlations are local in Fourier space, in which the kernel is

$$\tilde{\epsilon}(\mathbf{k}) = \frac{4a_s^2 N_{\text{cut}}}{\pi} e^{i|z|\mathbf{k}|/2} K_0 \left( \frac{|z|\mathbf{k}|}{2} \right), \quad (4)$$

where  $N_{\text{cut}} \equiv (e^{(\epsilon_{\text{cut}} - \mu)/(k_B T)} - 1)^{-1}$  is the number of reservoir atoms at the cutoff energy,  $K_0$  is a modified Bessel function of the second kind, and  $\sqrt{2}l_z$  is the  $1/e$  transverse “thickness” of the atomic cloud.

To derive a stochastic PV theory from Eq. (2), we exploit the fact that the energy-damping terms form a stochastic potential, and hence can be added to the GP action as potential energy terms, giving

$$S = \int \left( L_{\text{GP}} dt + \int d^2\mathbf{x} (V_\varepsilon dt - \hbar dU_\varepsilon) \rho \right), \quad (5)$$

where

$$L_{\text{GP}} = \int d^2\mathbf{x} \psi^* \left( i\hbar \partial_t + \frac{\hbar^2 \nabla^2}{2m} + \mu - \frac{g|\psi|^2}{2} \right) \psi \quad (6)$$

is the GP Lagrangian. That is, the variational (least action) theory obtained by minimizing the action functional (5) is precisely Eq. (2). This allows for an analytic treatment of vortex dynamics, provided a suitable ansatz is chosen for the classical field  $\psi$ .

We consider a system of isolated vortices on a homogeneous background, each with a single quantum of circulation  $\pm\hbar/m$ , for which the variational theory of the GP action reduces to the idealized PVM provided vortices are well separated [37], a condition satisfied by modern 2D vortex experiments in homogeneous systems which operate within the point-vortex regime [9–12,26,27]. In this case we can treat the nondissipative dynamics via the point-vortex Lagrangian [38]:

$$L_{\text{GP}} \approx L_{\text{PV}} \equiv 2\pi \hbar \rho_0 \left( \sum_n \frac{q_n}{2} \epsilon_{ij} \dot{X}_n^i X_n^j + \frac{\hbar}{m} \sum_{m \neq n} q_n q_m \log |\mathbf{r}_m - \mathbf{r}_n| \right), \quad (7)$$

where  $\epsilon_{ij}$  is the Levi-Civita symbol and  $\rho_0$  is the 2D background superfluid density.

Next, we integrate out the spatial degrees of freedom in the reservoir terms in Eq. (5) in order to express the action purely in terms of the vortex positions and velocities. Note that this requires only an appropriate ansatz for the 2D fluid density  $\rho$ , rather than the full classical field  $\psi$ . We choose a Gaussian ansatz for the density that separates the contribution of the vortices from the infinite background

$$\rho(\mathbf{x}, t) = \rho_0 \left( 1 - \sum_n e^{-|\mathbf{x} - \mathbf{r}_n(t)|^2 / 2\xi^2} \right), \quad (8)$$

where the healing length  $\xi$  gives the vortex core scale [39]. This ansatz is entirely characterized by microscopic parameters and has a Gaussian vortex core, which is needed for analytic tractability and provides an excellent approximation to the true vortex core in the region  $|\mathbf{x} - \mathbf{r}_n| \lesssim \xi$  – precisely where  $d\rho/dt$ , and hence dissipation described by Eq. (3), is most significant.

Next, since the Fourier transform of  $d\rho/dt$  is sharply peaked at the vortex core scale  $|\mathbf{k}| = \xi^{-1}$  for this density ansatz, we can treat the scattering kernel as approximately constant in Fourier space:  $\tilde{\varepsilon}(\mathbf{k}) \approx \tilde{\varepsilon}(\xi^{-1})$ . Consequently, we can write the scattering potential in the approximate local form

$$V_\varepsilon(\mathbf{x}) \approx 2N_{\text{cut}} \hbar \sigma_{\text{ED}} \frac{d\rho(\mathbf{x})}{dt}, \quad (9)$$

where  $\sigma_{\text{ED}} \equiv \sigma_s e^{l_z^2 / (2\xi)^2} K_0(l_z^2 / (2\xi)^2) / (2\pi)$  is an effective 2D scattering cross section for the energy-damping process in terms of the s-wave scattering cross section  $\sigma_s = 8\pi a_s^2$  [40]. A similar argument justifies treating the energy-damping noise correlator as approximately local in space (see Appendix C).

Under the above approximations, the spatial integrals over the damping term in Eq. (5) can be computed analytically to give

$$L_{\text{diss}} \equiv \int d^2\mathbf{x} V_\varepsilon(\mathbf{x}, t) \rho(\mathbf{x}, t) \quad (10)$$

$$= \sigma_{\text{ED}} N_{\text{cut}} \pi \hbar \rho_0^2 \sum_{nm} e^{-\frac{r_{nm}^2}{4\xi^2}} \hat{\mathbf{r}}_m \cdot (\mathbf{r}_m - \mathbf{r}_n), \quad (11)$$

where we have defined  $r_{nm}^2 \equiv |\mathbf{r}_n - \mathbf{r}_m|^2$ . Neglecting, for the moment, the noise term in Eq. (5), we can therefore derive dissipative dynamics of the point-vortex system by taking the Euler-Lagrange equations with respect to  $L_{\text{PV}} + L_{\text{diss}}$  (see Appendix C), which in the point-vortex limit of well-separated vortices  $r_{nm}^2 \gg \xi^2$  gives

$$\dot{\mathbf{r}}_n = \mathbf{v}_n^0 - \frac{\sigma_{\text{ED}} \rho_0 N_{\text{cut}} q_n}{2} \hat{\mathbf{z}} \times \dot{\mathbf{r}}_n$$

$$= \mathbf{v}_n^0 - \alpha_\varepsilon q_n \hat{\mathbf{z}} \times \mathbf{v}_n^0 + O(\alpha_\varepsilon^2), \quad (12)$$

where the last line is precisely the damped-PVM (1), with mutual friction coefficient

$$\alpha_\varepsilon \equiv \frac{\sigma_{\text{ED}} \rho_0 N_{\text{cut}}}{2}. \quad (13)$$

In Appendix D we compare the evolution of a vortex dipole under Eq. (12) to direct integration of the SPGPE (2), finding excellent quantitative agreement in the point-vortex limit  $r_{nm}^2 \gg \xi^2$ . This validates the two key approximations made in this derivation: our choice of density ansatz and approximate treatment of the energy-damping kernel.

The above calculation can be extended to include the noise term in Eq. (5), as the same set of approximations allow the spatial integrals arising in the noise correlations to be analytically computed. The full details of this computation are provided in Appendix C; the final result is the following stochastic point-vortex equation:

$$d\mathbf{r}_n = (\mathbf{v}_n^0 - \alpha_\varepsilon q_n \hat{\mathbf{z}} \times \mathbf{v}_n^0) dt + \sqrt{2\eta} d\mathbf{w}_n, \quad (14)$$

with leading corrections of order  $O(\alpha_\varepsilon^2, e^{-r_{nm}^2 / 4\xi^2}) \ll 1$ . Equation (14) is the key result of this work, describing not only vortex damping but also vortex diffusion driven by thermal fluctuations. The latter aspect is described by the noise vector  $d\mathbf{w}_n = (dW_n^x, dW_n^y, 0)$ , where  $dW_i^\alpha$  are Gaussian random variables with zero mean and correlations  $\langle dW_n^\alpha(t) dW_m^\beta(t') \rangle = \delta_{\alpha\beta} \delta_{nm} \delta(t - t') dt$ . The magnitude of the noise term is dictated by the diffusion coefficient, which is related to the mutual-friction coefficient by

$$\eta \equiv \alpha_\varepsilon \frac{k_B T}{2\pi \hbar \rho_0}. \quad (15)$$

The diffusive evolution can be interpreted as Brownian motion of vortices due to thermal fluctuations; further approximating the background flow with its average over the vortices, the

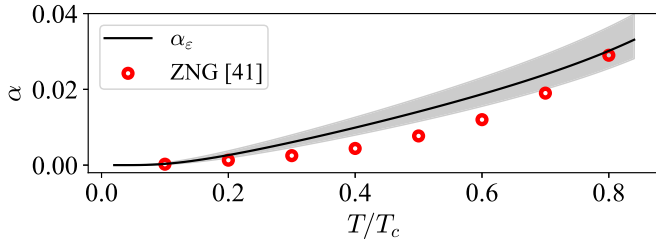


FIG. 2. Comparison of microscopic mutual friction  $\alpha_\epsilon$  (estimated with  $\epsilon_{\text{cut}} = 2\mu$ ) to mutual friction determined phenomenologically by fitting the damped PVM (1) to dynamical ZNG simulations [41]. We observe good quantitative agreement, with slight disagreement at intermediate temperatures. The microscopic prediction of  $\alpha$  varies slightly with the choice of energy cutoff; the shaded region denotes a 15% variation of  $\epsilon_{\text{cut}}$ .

convective position variance of each vortex grows diffusively:  $\langle \Delta \mathbf{r}_n^2 \rangle = 4\eta t$  (see Appendix E).

### Physical interpretation

The microscopic expression for the mutual friction coefficient (13) has a simple physical interpretation, as it is proportional to the product of the per-particle probability of energy-damping scattering  $\sigma_{\text{ED}}\rho_0$  and the number of thermal reservoir atoms at the cutoff  $N_{\text{cut}}$ . That is, the mutual friction coefficient is proportional to the rate of number-conserving two-body scattering events between the atoms in the condensed modes and atoms in the reservoir. It scales with both the number of reservoir atoms and condensed atoms, and recovers the idealized (nondissipative) PVM as  $T \rightarrow 0$ .

Additionally, the effective energy-damping cross section  $\sigma_{\text{ED}}$  is a monotonically decreasing function of the transverse thickness  $l_z$ , and thus so too is the mutual friction coefficient  $\alpha_\epsilon$ . Although the validity of the quasi-2D SPGPE requires  $l_z \lesssim \xi$ , we find our stochastic PV theory can quantitatively capture vortex damping in the much less restrictive regime  $l_z \lesssim 10\xi$ , consistent with previous work [42]. We demonstrate this in Fig. 2 by comparing our microscopic expression for the mutual friction coefficient to values phenomenologically extracted from Zaremba-Nikuni-Griffin (ZNG) kinetic theory simulations via fits to Eq. (1) [41]. There is excellent quantitative agreement with the fitted ZNG values of  $\alpha$ , despite the system considered in Ref. [41] having a significant 3D extent,  $l_z \sim 10\xi$ . Figure 2 also demonstrates that the value of  $\alpha_\epsilon$  does not strongly depend on the precise choice of  $\epsilon_{\text{cut}}$  (see Appendix F), varying weakly as  $\epsilon_{\text{cut}}$  is varied by 15%.

Although the SPGPE reservoir dissipation and noise terms satisfy the fluctuation-dissipation relation, this same relation does not apply for the damping and noise terms in the stochastic PV equation (14), as the thermal equilibrium of a nonrotating cloud corresponds to a system without vortices. As noted in Ref. [12], which used a stochastic PVM with experimentally fitted coefficients, the noise term in Eq. (14) is dissipative and can be understood as an effective viscosity term. Importantly, the microscopic formulas for  $\alpha_\epsilon$  and  $\eta$  provide a complete understanding of the relationship between thermal noise acting on vortices and the system temperature,

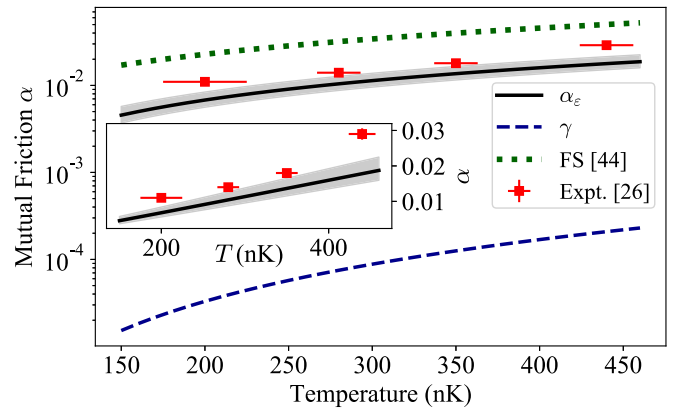


FIG. 3. Microscopic mutual friction contributions of number damping  $\alpha_\gamma = \gamma$  and energy damping  $\alpha_\epsilon$  (both estimated with  $\epsilon_{\text{cut}} = 2\mu$ ) compared to experimental measurements reported in Ref. [26]. Shaded region gives variation of  $\alpha_\epsilon$  for 15% change in  $\epsilon_{\text{cut}}$ . The number-damping estimate is several orders of magnitude smaller than the experimentally measured values; much closer agreement is given by the energy-damping estimate. The inset more clearly compares the experimental results to the energy-damping prediction, demonstrating agreement within  $\approx 20\%$ – $40\%$  of the experimentally measured values. For comparison, the analytical estimate of Ref. [44] disagrees with experiment by approximately a factor of two.

which under the phenomenological picture of mutual friction could only be obtained through *ad hoc* fitting.

Historically, a stochastic PVM of similar form to Eq. (14) was considered within the context of superfluid helium [8]. However, the inclusion of stochastic noise in Ref. [8] was not derived from microscopic theory, but motivated by fluctuation-dissipation arguments to generalize the phenomenological Hall-Vinen-Iordanskii equations [19,20,43]. Tractable microscopic models are lacking for superfluid helium, necessitating a phenomenological treatment of the damping that can only qualitatively describe experiment [21].

### IV. EXPERIMENTAL COMPARISON

Reference [26] reports experimental measurements of the mutual friction coefficient, obtained by fitting experimentally measured trajectories of a pair of like-sign vortices in a harmonic trap to the predictions of Eq. (1). Figure 3 compares these experimentally measured values to the analytic prediction of our microscopic model (13). For the temperature range considered in the experiment, the noise term in Eq. (14) is negligible ( $\eta \sim 10^{-5} \hbar/m$ ), despite strong damping.

Our microscopic prediction is within  $\sim 20\%$ – $40\%$  of the experimentally measured values; given the quoted thermal density variations of up to 30% and the linear dependence of  $\alpha_\epsilon \sim \rho_0$  [45], we do not expect agreement better than what we report here [46]. Harmonic trapping in the experiment also causes temperature-dependent vortex precession, which may further contribute to this discrepancy. In comparison, the mutual friction coefficient predicted from number-damping reservoir interactions ( $\alpha_\gamma = \gamma$ ) is several orders of magnitude smaller than the experimentally determined values, across the entire temperature range. This justifies the neglect of the number-damping process in our stochastic PV theory (14).

We may understand this result by noting the number-damping reservoir process drives equilibration against imbalance between the chemical potential of the low-energy atomic modes and the reservoir, which is significant during condensate growth. For vortex excitations in an otherwise equilibrated gas, which have a very low effective chemical potential, damping is therefore dominated by the number-conserving reservoir process which directly opposes changes in the atomic density.

Our microscopic prediction also gives closer quantitative agreement than the theoretical estimate of  $\alpha \approx (n_{\text{th}}/n_0)\sqrt{\mu/(k_B T)}$  by Ref. [44], where  $n_{\text{th}}/n_0$  is the ratio of the 3D densities of the thermal cloud and condensate, respectively. This estimate is derived from low-energy perturbation theory and can only be phenomenologically extended to compare to the experiment of Ref. [26], where a significant thermal fraction was present.

The close quantitative agreement between our microscopic prediction  $\alpha_\varepsilon = \sigma_{\text{ED}}\rho_0 N_{\text{cut}}/2$  and this experiment confirms that energy-damping reservoir interactions are the underlying microscopic mechanism to mutual friction in 2D atomic superfluids. Consequently, previous modeling of thermal friction in 2D quantum vortices that neglected energy damping must be treated as phenomenological. It will therefore be important to revisit previous microscopic 2DQT modeling, such as in Ref. [47], and make quantitative predictions with the explicit inclusion of energy-damping interactions.

## V. APPLICATION OF THEORY: VORTEX DIFFUSIVITY AT THE BKT TRANSITION

At higher temperatures near the transition to superfluidity, vortex diffusion driven by critical thermal fluctuations is expected to play a more significant role. In particular, the diffusion coefficient  $\eta$  is an essential parameter in dynamic corrections to static BKT theory [8,48,49], yet it is currently treated as a phenomenological fitting parameter in the context of ultracold atomic gases [50]. Our work provides a microscopic expression for  $\eta$  and sets a theoretical foundation for future experiments probing the BKT regime. For example, we can predict the value of  $\eta$  for a weakly interacting Bose gas at the BKT transition temperature  $T_c^{\text{BKT}} = 2\pi\rho_0\hbar^2/[mk_B \ln(360/\tilde{g})]$  [51], where  $\tilde{g} = \sqrt{8\pi}a_s/l_z$ . For typical experimental parameters (e.g., Ref. [52]), our microscopic expression predicts  $\eta \sim 10^{-2}\hbar/m$  at the BKT transition—two orders of magnitude smaller than in strongly interacting superfluid helium films [8,48].

## VI. CONCLUSION

We have provided a microscopic foundation for mutual friction and thermal diffusion of 2D vortex motion in atomic superfluids, based on often neglected finite-temperature interactions with a static thermal reservoir. We derived a stochastic point-vortex theory, which gives an analytic expression for the mutual friction coefficient that compares excellently with available experimental data. The damped evolution in this theory is consistent with previous phenomenological modeling, validating the mutual friction concept in studies of turbulent atomic superfluids. These results profoundly impact future

theory of vortex dynamics in atomic superfluids, showing the importance of energy-damping interactions for quantitative understanding of dissipation. Crucially, our microscopic theory allows experimentally testable predictions of 2D quantum vortex dynamics without any fitted parameters.

2DQT experiments have evolved significantly and now routinely study 2D vortex dynamics in homogeneous systems [9–12,27], allowing further tests of our theory. In particular, experimentally measuring the diffusion coefficient  $\eta$  is an important test of stochastic point-vortex theory. In principle,  $\eta$  can be extracted from the dynamics of a corotating pair of same-sign vortices by tracking the drift in their center-of-mass position. The thermal noise identified sets a floor for the total noise that will include other sources, such as technical noise in the trapping potential and incoherent density fluctuations. Observing the fundamental point-vortex noise poses an interesting challenge for future experimental study, and an important test of BKT physics in ultracold gases.

A deeper understanding of thermal friction's role in quantum turbulence could require further theoretical investigations into the effect of reservoir interactions on vortex dynamics outside of the point-vortex regime, for which a numerical approach will probably be required. Beyond its influence on vortex core motion, energy damping will also couple strongly to compressible excitations [53,54], with important implications for weak-wave turbulence in quantum fluids [55,56].

## ACKNOWLEDGMENTS

We acknowledge insightful discussions with John Close, Tyler Neely, and Matthew Reeves. This research was undertaken with the assistance of resources and services from the National Computational Infrastructure (NCI), which is supported by the Australian Government. Z.M. is supported by an Australian Government Research Training Program (RTP) Scholarship. A.S.B. acknowledges financial support from the Marsden Fund (Grant No. 17-UOO-028) and the Dodd-Walls Centre for Photonic and Quantum Technologies. S.S.S. is supported by an Australian Research Council Discovery Early Career Researcher Award (DECRA), Project No. DE200100495.

## APPENDIX A: BRIEF REVIEW OF SPGPE THEORY

The SPGPE is a first-principles reservoir theory that quantitatively describes a finite-temperature ultracold Bose gas [24]. Within this framework, highly populated modes of the quantum field (generally  $\gtrsim 1$  atoms on average) are treated as a coherent classical field  $\psi$ , which interacts with an incoherent thermal reservoir composed of the remaining sparsely occupied high-energy modes. This leads to a stochastic equation of motion for the classical field  $\psi$ , which in Stratonovich form is

$$i\hbar d\psi(\mathbf{r}, t) = \mathcal{P}[(1 - i\gamma)(\mathcal{L} - \mu)\psi dt + V_\varepsilon(\mathbf{r}, t)\psi dt + i\hbar d\xi_\gamma(\mathbf{r}, t) - \hbar\psi dU_\varepsilon(\mathbf{r}, t)], \quad (\text{A1})$$

where  $\mathcal{L} = H_0 + g|\psi|^2$  for the single-particle Hamiltonian  $H_0$ . Here  $g = 4\pi a_s \hbar^2/m$  is the two-body interaction strength for an s-wave scattering length  $a_s$ . The explicit inclusion of the projector  $\mathcal{P}$  ensures dynamic separation of the field into a low-energy coherent region and incoherent reservoir. The

noise terms  $d\xi_\gamma$  and  $dU_\varepsilon$  correspond to incoherent thermal fluctuations from the number-damping and energy-damping processes, respectively, and coupled with the deterministic dissipation terms ultimately drive any initial state to a steady state at thermal equilibrium within the grand-canonical ensemble at temperature  $T$  and chemical potential  $\mu$ . The strengths of the number-damping and energy-damping dissipation processes are characterized by the dimensionless quantity  $\gamma$  and the length-squared quantity  $\mathcal{M}$ , respectively. These parameters can be *a priori* determined from the reservoir chemical potential  $\mu$ , temperature  $T$ , and the energy cutoff  $\varepsilon_{\text{cut}}$  [29]:

$$\gamma = \frac{8a_s^2}{\lambda_{\text{dB}}^2} \sum_{j=1}^{\infty} \frac{e^{\beta\mu(j+1)}}{e^{2\beta\varepsilon_{\text{cut}}j}} \Phi[e^{\beta(\mu-2\varepsilon_{\text{cut}})}, 1, j], \quad (\text{A2})$$

$$\mathcal{M} = \frac{16\pi a_s^2}{\exp\left(\frac{\varepsilon_{\text{cut}}-\mu}{k_B T}\right) - 1}, \quad (\text{A3})$$

where  $a_s$  is the s-wave scattering length,  $\beta = 1/(k_B T)$ ,  $\lambda_{\text{dB}} = \sqrt{2\pi\hbar^2/(mk_B T)}$  is the thermal de Broglie wavelength, and  $\Phi[z, x, a]$  is the Lerch transcendent.

In the main text, we define  $N_{\text{cut}} \equiv (e^{(\varepsilon_{\text{cut}}-\mu)/(k_B T)} - 1)^{-1}$  as the number of reservoir atoms at the cutoff energy, as it is the thermal equilibrium number distribution for an ideal gas evaluated at the cutoff energy. This is a good estimate of the true number of atoms at the cutoff energy, as the cutoff energy  $\varepsilon_{\text{cut}}$  should be sufficiently large compared to  $\mu$  such that high-energy modes very close to the cutoff are essentially noninteracting (see the discussion in Appendix F). The energy-damping coefficient can then be written as  $\mathcal{M} = 2\sigma_s N_{\text{cut}}$ , where  $\sigma_s \equiv 8\pi a_s^2$  is s-wave scattering cross section.

The energy-damping dissipation process is described by an effective potential term  $V_\varepsilon$ :

$$V_\varepsilon(\mathbf{r}, t) = -\hbar \int d^3\mathbf{r}' \varepsilon_{3D}(\mathbf{r} - \mathbf{r}') \nabla_{\mathbf{r}'} \cdot \mathbf{j}(\mathbf{r}', t), \quad (\text{A4})$$

which is a convolution between the divergence of the particle current  $\mathbf{j}(\mathbf{r}, t)$  and the scattering kernel

$$\varepsilon_{3D}(\mathbf{r}) = \frac{\mathcal{M}}{(2\pi)^3} \int d^3\mathbf{k} \frac{e^{i\mathbf{k}\cdot\mathbf{r}}}{|\mathbf{k}|}. \quad (\text{A5})$$

The noise terms in the SPGPE are random Gaussian variables with zero mean and correlations:

$$\langle d\xi_\gamma^*(\mathbf{r}, t) d\xi_\gamma(\mathbf{r}', t') \rangle = \frac{2\gamma k_B T}{\hbar} \delta(\mathbf{r} - \mathbf{r}') \delta(t - t') dt, \quad (\text{A6})$$

$$\langle dU_\varepsilon(\mathbf{r}, t) dU_\varepsilon(\mathbf{r}', t') \rangle = \frac{2k_B T}{\hbar} \varepsilon_{3D}(\mathbf{r} - \mathbf{r}') \delta(t - t') dt. \quad (\text{A7})$$

Note that the number-damping noise  $d\xi_\gamma$  is complex, whereas the energy-damping noise  $dU_\varepsilon$  is real-valued.

To zeroth order in the reservoir processes, the SPGPE satisfies the continuity equation

$$\nabla \cdot \mathbf{j} + \frac{\partial \rho}{\partial t} = 0, \quad (\text{A8})$$

where  $\rho = |\psi|^2$  is the fluid density (the leading correction occurs at order  $\gamma \ll 1$ ). Crucially, the above relation remains exactly satisfied by the energy-damping reservoir process, with corrections only coming in through the number-damping interaction terms. Therefore for the derivation presented in

the main text, where we neglect the number-damping process, the energy-damping potential directly opposes changes in the density:

$$V_\varepsilon(\mathbf{r}, t) dt = \hbar \int d^3\mathbf{r}' \varepsilon(\mathbf{r} - \mathbf{r}') d\rho(\mathbf{r}', t). \quad (\text{A9})$$

## APPENDIX B: QUASI-2D SPGPE AND THE EFFECTIVE SCATTERING KERNEL

For studies of 2D systems, it is convenient to work with a quasi-2D form of the SPGPE, where the transverse ( $z$ ) degrees of freedom are integrated out. In the case of 2D vortex dynamics, this requires only that the transverse length scale be of the same order as the healing length  $l_z \approx O(\xi)$ , which ensures that Kelvin waves along the vortex filaments are suppressed [42]. This is a much less restrictive condition than the oblate confinement need to realize a thermodynamically 2D gas (i.e., the BKT transition), thus the quasi-2D SPGPE can be used to investigate 2D vortex dynamics in a convenient regime where condensate fraction, temperature, etc., are all well defined [57].

The resulting quasi-2D SPGPE has the same form as Eq. (A1) with the following modified 2D scattering kernel [33]:

$$\varepsilon(\mathbf{x}) = \frac{1}{2\pi} \int d^2\mathbf{k} e^{i\mathbf{k}\cdot\mathbf{x}} \underbrace{\left[ \frac{\mathcal{M}}{(2\pi)^2} F\left(\frac{l_z |\mathbf{k}|^2}{4}\right) \right]}_{\tilde{\varepsilon}(\mathbf{k})}, \quad (\text{B1})$$

where  $F(x) = e^x K_0(x)$  with  $K_0$  a modified Bessel function of the second kind, and  $\mathcal{M} = 16\pi a_s^2 [\exp(\frac{\varepsilon_{\text{cut}}-\mu}{k_B T}) - 1]^{-1}$ .

The convolution with the scattering kernel in the energy-damping potential given in Eq. (3) adds a level of complexity that prevents most integrals involving  $V_\varepsilon$  to be analytically solved. In the main text we treat this by approximating the kernel as flat in Fourier space, evaluated at the vortex core scale  $k = \xi^{-1}$ . This results in a simplified form of the kernel:

$$\varepsilon(\mathbf{x}) \approx 2\pi \tilde{\varepsilon}(\xi^{-1}) \delta(\mathbf{x}) = 2\sigma_{\text{ED}} N_{\text{cut}} \delta(\mathbf{x}), \quad (\text{B2})$$

where  $\sigma_{\text{ED}} = \sigma_s F(\frac{l_z^2}{4\xi^2})/(2\pi)$  is the effective energy-damping scattering cross section defined in the main text, and the factor of  $2\pi$  in the first line arises due to the convolution theorem for the 2D Fourier transform (in the unitary transform convention).

## APPENDIX C: DETAILED DERIVATION OF EQ. (14)

Here we provide further details of the derivation of the stochastic point-vortex equation [Eq. (14)] from the variational action formulation of the quasi-2D SPGPE [Eq. (5)] and the approximate form of the energy-damping kernel described in Appendix B.

As described in the main text, the spatial degrees of freedom can be integrated out from the energy-damping reservoir terms in the action with an appropriate ansatz for the 2D fluid density  $\rho$  in terms of the vortex positions  $\mathbf{r}_n(t)$ . In Fig. 4 we demonstrate that our Gaussian ansatz for the density

$$\rho(\mathbf{x}, t) = \rho_0 \left[ 1 - \sum_n \exp\left(-\frac{|\mathbf{x} - \mathbf{r}_n(t)|^2}{2\xi^2}\right) \right] \quad (\text{C1})$$

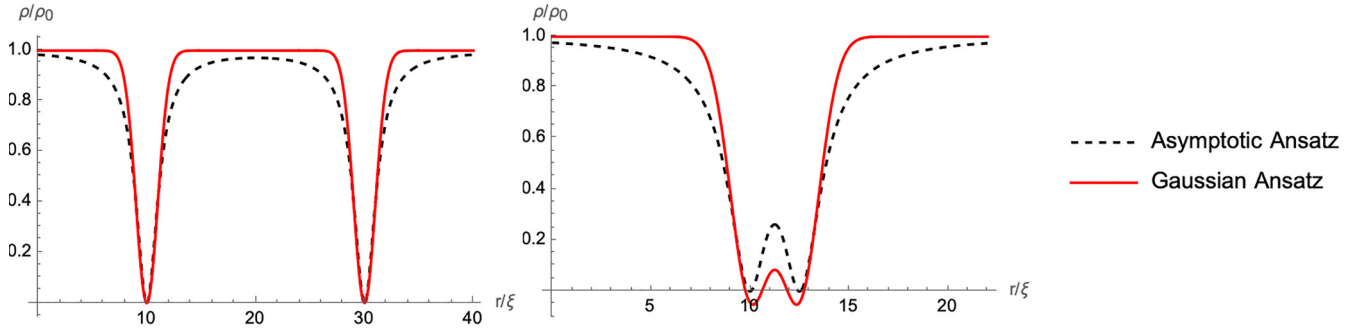


FIG. 4. Comparison of the Gaussian density ansatz (C1) (red) to the analytic asymptotic solution  $\rho(\mathbf{x}) \approx \rho_0 \prod_n |\mathbf{x} - \mathbf{r}_n|^2 / (|\mathbf{x} - \mathbf{r}_n|^2 + 0.82^{-2})$  [57] (black, dashed), for a pair of well-separated vortices (left) and vortices separated by  $2.5\xi$  (right). For the former case, the ansatz is an excellent description of density within  $1\xi$  of the vortex cores and is positive definite. In the latter case, the density becomes slightly negative as there is significant overlap between the two vortex cores.

agrees well with the exact GPE solution for a single vortex core in the range  $|\mathbf{x} - \mathbf{r}_n(t)| \lesssim \xi$ . Furthermore, Fig. 4 illustrates that, although this ansatz is not strictly nonnegative in the multivortex case, it is well approximated as such in the point-vortex regime where vortices are well separated. The form of this ansatz is convenient for this derivation for two key reasons: (1) the Gaussian form allows for simple analytic computation of the spatial integrals in Eq. (5), and (2) the infinite background term does not need to be manually discarded, as only derivatives of the density contribute to the final equation of motion.

First, we focus on the dynamics generated by damping term in the Lagrangian  $L_{\text{diss}}$ , given in Eq. (11), neglecting the noise term in Eq. (5) for now. Taking the Euler-Lagrange equations with respect to  $L_{\text{PV}} + L_{\text{damping}}$ , we have

$$\begin{aligned} q_n \left[ \begin{pmatrix} -\dot{Y}_n \\ \dot{X}_n \end{pmatrix} + \frac{\hbar}{m} \sum_{m \neq n} \frac{q_m}{r_{mn}^2} \begin{pmatrix} \delta x_{nm} \\ \delta y_{nm} \end{pmatrix} \right] \\ = \frac{\alpha_\varepsilon}{2\xi^2} \sum_m e^{-\frac{\gamma_{mn}}{4\xi^2}} \begin{pmatrix} \dot{X}_m (2\xi^2 - \delta x_{mn}^2) - \dot{Y}_m \delta x_{mn} \delta y_{mn} \\ \dot{Y}_m (2\xi^2 - \delta y_{mn}^2) - \dot{X}_m \delta x_{mn} \delta y_{mn} \end{pmatrix}, \end{aligned}$$

where we have canceled common factors of  $2\pi\hbar\rho_0$ , and used the definition  $\alpha_\varepsilon \equiv \sigma_{\text{ED}}\rho_0 N_{\text{cut}}/2$ . In the point-vortex limit  $r_{mn}^2 \gg \xi^2$ , we may make the approximation  $\exp[-r_{mn}^2/(4\xi^2)] \approx \delta_{mn}$ , resulting in a very simple set of equations:

$$\begin{pmatrix} \dot{X}_n \\ \dot{Y}_n \end{pmatrix} \approx \frac{\hbar}{m} \sum_{m \neq n} \frac{q_m}{r_{mn}^2} \begin{pmatrix} -\delta y_{nm} \\ \delta x_{nm} \end{pmatrix} + \frac{\alpha_\varepsilon}{q_n} \begin{pmatrix} \dot{Y}_n \\ -\dot{X}_n \end{pmatrix}.$$

Since the first term on the right-hand side is exactly the background superfluid velocity at the  $i$ th vortex  $\mathbf{v}_i^0$ , we may write this equation as (assuming  $q_n = \pm 1$ ):

$$\begin{aligned} \dot{\mathbf{r}}_n &= \mathbf{v}_n^0 - \alpha_\varepsilon q_n \hat{\mathbf{z}} \times \dot{\mathbf{r}}_n \\ &= \mathbf{v}_n^0 - \alpha_\varepsilon q_n \hat{\mathbf{z}} \times \mathbf{v}_n^0 + O(\alpha_\varepsilon^2), \end{aligned} \quad (\text{C2})$$

where in the last line we substituted in the zeroth-order result  $\dot{\mathbf{r}}_n = \mathbf{v}_n^0 + O(\alpha_\varepsilon)$ . This gives Eq. (12).

Next, we derive the noise term in the stochastic point-vortex equation (14) and its correlations, starting from the

noise term in Eq. (5):

$$S_{\text{noise}} \equiv -\hbar \int d^2\mathbf{x} \rho(\mathbf{x}, t) \int dU_\varepsilon(\mathbf{x}, t). \quad (\text{C3})$$

In contrast to the approach for the damping term, we will find it convenient to evaluate the spatial integrals after first taking the Euler-Lagrange equations with respect to the vortex positions. The above noise term contributes the following term to the equations of motion:

$$\left. \begin{pmatrix} dX_n \\ dY_n \end{pmatrix} \right|_{\text{noise}} = d\mathbf{U}_n(t), \quad (\text{C4})$$

where we have defined the stochastic noise vector

$$d\mathbf{U}_n(t) \equiv \frac{1}{2\pi\rho_0 q_n} \int d^2\mathbf{x} dU_\varepsilon(\mathbf{x}, t) \begin{pmatrix} -(\partial\rho(\mathbf{x})/\partial Y_n) \\ (\partial\rho(\mathbf{x})/\partial X_n) \end{pmatrix}.$$

We will now consider the noise correlations of this stochastic noise vector using the properties of  $dU_\varepsilon$  given in the main text. To simplify our expressions, we denote the  $i$ th element of the vectors  $d\mathbf{U}_n(t)$  and  $\mathbf{r}_n = (X_n, Y_n)^T$  by  $dU_n^i(t)$  and  $X_n^i$ , respectively, and define  $\sigma^{ij} = 1$  if  $i = j$  and  $\sigma^{ij} = -1$  if  $i \neq j$ .

Following from the properties of  $dU_\varepsilon$ ,  $d\mathbf{U}_n(t)$  is a Gaussian noise vector with zero mean and correlations:

$$\begin{aligned} \langle dU_n^i(t) dU_m^j(t') \rangle &= \frac{\sigma^{ij}}{(2\pi\rho_0)^2} \int d^2\mathbf{x} \int d^2\mathbf{y} \frac{\partial\rho(\mathbf{x})}{\partial X_n^i} \frac{\partial\rho(\mathbf{y})}{\partial X_m^j} \\ &\quad \times \langle dU_\varepsilon(\mathbf{x}, t) dU_\varepsilon(\mathbf{y}, t') \rangle, \quad (\text{C5a}) \\ &= \frac{2k_B T \sigma^{ij}}{\hbar(2\pi\rho_0)^2} \delta(t - t') \int d^2\mathbf{x} \frac{\partial\rho(\mathbf{x})}{\partial X_n^i} \\ &\quad \times \left( \int d^2\mathbf{y} \frac{\partial\rho(\mathbf{y})}{\partial X_m^j} \varepsilon(\mathbf{x} - \mathbf{y}) \right) dt. \quad (\text{C5b}) \end{aligned}$$

The integrand of the bracketed integral in Fourier space is a local product of the Fourier transform of  $\partial\rho/\partial X_m^j$  and the kernel  $\tilde{\varepsilon}(\mathbf{k})$ . Following the same argument made in the main text for the energy-damping potential term, we may approximate this integral by noting  $\partial\rho/\partial X_m^j$  will be peaked in Fourier space at  $k = \xi^{-1}$ , allowing us to treat the kernel as

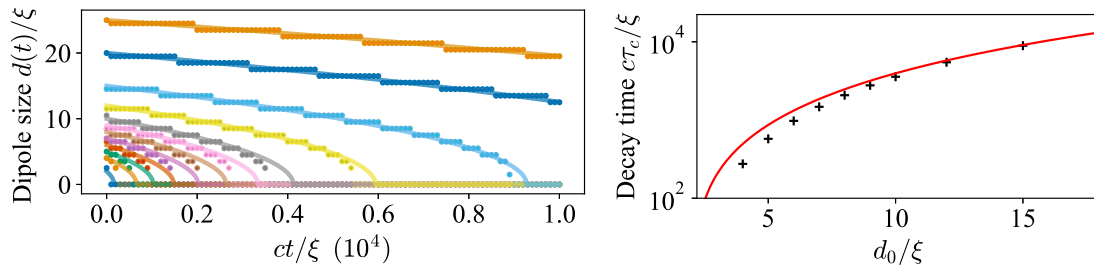


FIG. 5. Numerical validation of the damped point-vortex model for dipole decay. (a) Dipole size as a function of time for various initial sizes  $d_0 \in [2, 25]\xi$  as given by the analytic expression Eq. (D1) (lines) and numerical integration of the noiseless SPGPE (pluses). (b) Decay time  $\tau_c$ , defined as  $d(\tau_c) = d_c$  for  $d_c = 2\xi$ , given in terms of the speed of sound  $c = \sqrt{\mu/m}$ , as a function of initial dipole size  $d_0 \in [4, 15]\xi$ . Analytic expression (D1) compares well to numeric values, with increasing agreement for  $d \gg d_c$ .

constant at this scale:  $\tilde{\varepsilon}(\mathbf{k}) \approx \tilde{\varepsilon}(\xi^{-1})$ . This allows us to make the substitution (B2) in the above correlation,

$$\begin{aligned} \langle dU_n^i(t)dU_m^j(t') \rangle &\approx \sigma^{ij} \frac{4k_B T \sigma_{\text{ED}} N_{\text{cut}}}{\hbar(2\pi\rho_0)^2} \delta(t-t') dt \\ &\times \int d^2\mathbf{x} \frac{\partial\rho(\mathbf{x})}{\partial X_n^i} \int d^2\mathbf{y} \frac{\partial\rho(\mathbf{y})}{\partial X_m^j} \delta(\mathbf{x}-\mathbf{y}), \\ &= \sigma^{ij} \frac{k_B T \sigma_{\text{ED}} N_{\text{cut}}}{\pi^2 \hbar \rho_0^2} \delta(t-t') dt \\ &\times \int d^2\mathbf{x} \frac{\partial\rho(\mathbf{x})}{\partial X_n^i} \frac{\partial\rho(\mathbf{x})}{\partial X_m^j}. \end{aligned}$$

The integral can be solved analytically for our choice of density ansatz

$$\begin{aligned} \int d^2\mathbf{x} \frac{\partial\rho(\mathbf{x})}{\partial X_n^i} \frac{\partial\rho(\mathbf{x})}{\partial X_m^j} &= \frac{\pi\rho_0^2 e^{-\frac{r_{mn}^2}{4\xi^2}}}{4\xi^2} (2\xi^2 \delta_{ij} - \delta X_{mn}^i \delta X_{mn}^j) \\ &\approx \frac{\pi\rho_0^2}{2} \delta_{ij} \delta_{nm}, \end{aligned} \quad (\text{C7})$$

where in the last step we have again made the approximation  $\exp[-r_{mn}^2/(4\xi^2)] \approx \delta_{mn}$  valid in the point-vortex regime  $r_{mn}^2 \gg \xi^2$ . Therefore, off-diagonal correlations vanish, leading to the simple expression

$$\langle dU_n^i(t)dU_m^j(t') \rangle = 2 \frac{\alpha_\varepsilon k_B T}{2\pi \hbar \rho_0} \delta_{ij} \delta_{nm} \delta(t-t') dt, \quad (\text{C8})$$

noting  $\sigma^{ij} \delta_{ij} = \delta_{ij}$  and  $\sigma_{\text{ED}} N_{\text{cut}} = 2\alpha_\varepsilon/\rho_0$ . This correlation allows us to express the noise vector in terms of white noise processes:

$$d\mathbf{U}_n(t) \equiv \sqrt{2\eta} d\mathbf{w}_n(t) = \sqrt{2\eta} \begin{pmatrix} dW_n^x(t) \\ dW_n^y(t) \end{pmatrix}, \quad (\text{C9})$$

where  $dW_n^i$  are real Gaussian noises with zero mean and correlation  $\langle dW_n^i(t)dW_m^j(t') \rangle = \delta_{ij} \delta_{nm} dt$  (i.e., Weiner increments), and we have defined the diffusion coefficient (units  $\text{length}^2/\text{time}$ ):  $\eta \equiv \alpha_\varepsilon k_B T / (2\pi \hbar \rho_0)$ . This gives the noise term in Eq. (14).

#### APPENDIX D: NUMERIC VALIDATION: DIPOLE DECAY AND DENSITY ANSATZ

Here we numerically validate our choice of density ansatz and approximate treatment of the energy-damping kernel  $\varepsilon(\mathbf{x}) \approx 2\sigma_{\text{ED}} N_{\text{cut}} \delta(\mathbf{x})$  by comparing the predictions of our derived point-vortex equation against direct integration of the quasi-2D SPGPE [with the exact expression for the scattering kernel  $\varepsilon(\mathbf{x})$ ] for a vertical thickness of  $l_z = \xi$ . For simplicity, we neglect the noise in both equations, effectively comparing the predictions of each equation for the *mean* vortex dynamics. This allows us to separate deviations due to the approximate form of the kernel and density (used in both the damping and noise terms) from sampling errors in averaging over a finite number of stochastic trajectories.

Specifically, we consider the decay of a vortex-antivortex dipole due to damping, for which the analytic solution to the damped point-vortex equation is well-known (see, for example, Ref. [27]). For our model, this solution can be written as

$$d(t) = \sqrt{d(0)^2 - 4 \frac{\hbar}{m} \alpha_\varepsilon t}, \quad (\text{D1})$$

where  $d(t)$  is the separation between the two vortices and we have neglected the contribution of number damping. By defining a critical scale  $d_c$  at which the vortex-antivortex pair are expected to annihilate, we can estimate a timescale for decay  $\tau_c = m[d(0)^2 - d_c^2]/(4\hbar\alpha_\varepsilon)$ . An estimate of this critical scale is  $d_c = 2\xi$ , where  $\xi$  is the healing length of the fluid [27]. Our simulations are performed in dimensionless healing length units of  $\xi$  (space) and  $c/\xi = \hbar/\mu$  (time), with  $l_z = \xi$  and  $\mathcal{M} = 2\sigma_{\text{ED}} N_{\text{cut}} \rho_0 = 0.1$  together giving a mutual friction coefficient  $\alpha_\varepsilon \approx 0.006$ . Here  $c = \sqrt{\mu/m}$  is the speed of sound in the superfluid.

Figure 5 compares the analytic expression Eq. (D1) to direct numerical integration of the noiseless quasi-2D SPGPE (with  $\gamma = 0$ ) for a range of initial dipole sizes. We see strong quantitative agreement between the analytic and numeric results, particularly for large intervortex distances  $d(t) \gg \xi$ . This clearly demonstrates the validity of the assumptions made in the derivation of our model in the point-vortex limit (e.g., the density ansatz and the approximate form of the kernel), and the stability of our model over long timescales. We observe growing discrepancy between the analytics for dipole



sizes below  $d(t) \lesssim 5\xi$ , indicating the expected breakdown of a point-vortex description of the vortex dynamics. When the approximate form of the energy-damping kernel is also used in the numeric simulations, we observe a slight improvement in the agreement for dipoles with initial separation  $d(0) \lesssim 10\xi$ . This demonstrates that there is a weak quantitative deviation due to the density ansatz and treatment of the kernel, but only close to the breakdown of the point-vortex regime.

### APPENDIX E: BROWNIAN MOTION IN THE MEAN-FIELD APPROXIMATION

Here we show that the convective position variance of each vortex grows diffusively under the evolution of Eq. (14) in the mean-field limit. Specifically we consider the mean-field approximation wherein each vortex interacts with a mean-field flow induced by all other vortices, allowing us to approximate Eq. (14) by

$$d\mathbf{r}_n = \langle \mathbf{v}_n^0 - \alpha_\varepsilon q_n \hat{\mathbf{z}} \times \mathbf{v}_n^0 \rangle dt - \sqrt{2\eta} d\mathbf{w}_n, \quad (\text{E1})$$

where we have replaced the background superfluid velocity at the  $i$ th vortex,  $\mathbf{v}_i^0$ , with its stochastic average  $\langle \mathbf{v}_i^0 \rangle$ . In other words, under this assumption the  $i$ th vortex interacts with the mean velocity field produced by the dynamics of all other vortices.

Using the shorthand  $\langle \mathbf{v}_i^0 \rangle - \alpha_\varepsilon q_i \hat{\mathbf{z}} \times \langle \mathbf{v}_i^0 \rangle \equiv (a_i(t), b_i(t), 0)^T$ , we can then write the solution of the above equation as a vector Ornstein-Uhlenbeck process:

$$X_i(t) = x_0 + \int_0^t a_i(t') dt' - \sqrt{2\eta} \int_0^t dW_i^x(t'), \quad (\text{E2a})$$

$$Y_i(t) = y_0 + \int_0^t b_i(t') dt' + \sqrt{2\eta} \int_0^t dW_i^y(t'). \quad (\text{E2b})$$

From here we may then compute the variance of the positions by noting that the noise vanishes in the means ( $\langle dW_i^\alpha \rangle = 0$ ):

$$\langle \Delta X_i^2 \rangle \equiv \langle (X_i(t) - \langle X_i(t) \rangle)^2 \rangle \quad (\text{E3})$$

$$= 2\eta \int_0^t dt' \int_0^t dt'' \langle dW_i^x(t') dW_i^x(t'') \rangle \quad (\text{E4})$$

$$= 2\eta \int_0^t dt' = 2\eta t. \quad (\text{E5})$$

An identical calculation gives  $\langle Y_i^2 \rangle = 2\eta t$ . Finally, this allows us to compute the growth of the variance induced by thermal fluctuations, in the mean-field approximation:

$$\langle \Delta r_i^2 \rangle \equiv \langle \Delta X_i^2 + \Delta Y_i^2 \rangle = 4\eta t. \quad (\text{E6})$$

This can be interpreted as Brownian motion of vortices around the background flow, with diffusive growth of the position variance of each vortex.

### APPENDIX F: DETERMINATION OF THE ENERGY CUTOFF

Determining the value of the energy cutoff  $\epsilon_{\text{cut}}$  for a particular experiment is a nontrivial yet essential aspect of first-principles modeling with the SPGPE. To ensure the validity of the SPGPE framework, the choice of cutoff must

satisfy two key properties. First,  $\epsilon_{\text{cut}}$  must be chosen such that each of the modes in the low-energy region are appreciably occupied, i.e., have occupation no fewer than  $O(1)$  atoms [24]. Second, the cutoff should be sufficiently large (compared to  $\mu$ ) to ensure the interacting modes of the system are contained within the low-energy coherent region. The latter requirement is typically satisfied for  $\epsilon_{\text{cut}} \gtrsim 2\mu$  [58], where  $\mu$  is the chemical potential of the reservoir.

These constraints do not uniquely specify a particular energy cutoff, but rather tightly constrains appropriate choices of  $\epsilon_{\text{cut}}$ . In principle, this means calculations in the SPGPE framework will depend weakly on the precise choice of  $\epsilon_{\text{cut}}$ . In practice, it is therefore important for first-principles SPGPE calculations to demonstrate robustness of results to small variations of  $\epsilon_{\text{cut}}$  (on the order of 10%); see, for example, Refs. [5,24,29,34]. In the main text results are shown for a 15% variation in  $\epsilon_{\text{cut}}$ .

For the comparison to Ref. [26] presented in Fig. 3, we find the choice of  $\epsilon_{\text{cut}} = 2\mu$  to satisfy the two requirements described above, across the temperature range considered. Significantly increasing the cutoff beyond this value results in the highest-energy modes becoming too sparsely occupied, particularly for the lower range of temperatures considered. For example, setting  $\epsilon_{\text{cut}} = 3\mu$  results in  $N_{\text{cut}} \approx 0.4$  for the  $T = 200$  nK in Fig. 3. Significantly reducing the cutoff below  $2\mu$  will result in a number of appreciably occupied interacting modes of the system inappropriately becoming part of the incoherent region.

### APPENDIX G: ESTIMATION OF ATOMIC CLOUD PARAMETERS

#### 1. Reduction to 2D theory: Calculation of $l_z$ , $\mu_{2D}$ , $\rho_0$ from 3D cloud parameters

A key parameter in our stochastic point vortex theory is the vertical thickness of the atomic cloud  $l_z$ . In terms of the quasi-2D SPGPE, this is defined as the  $1\sigma$  radius of the transverse wavefunction, which is treated as a Gaussian [33]. In this work we compute  $l_z$  for a given harmonically trapped system based on the analytical variational ground state for a Gaussian ansatz, as given in Ref. [40]. Specifically, we find  $l_z$  as the solution to the following algebraic equation [ $b_i = l_i / \sqrt{\hbar/(m\omega_i)}$ ]:

$$\frac{1}{2} \hbar \omega_i \left( b_i^2 - \frac{1}{b_i^2} \right) - \frac{1}{2(2\pi)^{3/2}} \frac{gN_0}{l_{\text{geo}}^3} \frac{1}{b_1 b_2 b_3} = 0, \quad (\text{G1})$$

where  $\omega_{\text{geo}} = (\omega_x \omega_y \omega_z)^{1/3}$  is the geometric mean of the trapping frequencies,  $l_{\text{geo}} = \sqrt{\hbar/(m\omega_{\text{geo}})}$ , and  $N_0$  is the number of condensate atoms.

Integrating out the  $z$  dimension results in an effective 2D chemical potential and interaction strength:

$$\mu_{2D} = \mu - \frac{m\omega_z^2 l_z^2}{4} - \frac{\hbar^2}{4ml_z^2}, \quad (\text{G2})$$

$$g_{2D} = \frac{g}{\sqrt{2\pi} l_z}, \quad (\text{G3})$$

which we use to estimate the healing length  $\xi = \hbar/\sqrt{m\mu_{2D}}$  and the 2D background density  $\rho_0 = \mu_{2D}/g_{2D}$ .

## 2. Estimation of chemical potential for comparison to ZNG simulations of Ref. [41]

In the main text, we compare our microscopically derived expression for the mutual friction coefficient to the numerical calculations of Ref. [41]. In their calculations, the total atom number  $N_T$  of the gas was fixed for all temperatures studied, resulting in a different chemical potential for each temperature considered, therefore changing the effective energy cutoff for each temperature. For each temperature  $T$ , we compute the chemical potential by first estimating the number of condensate atoms  $N_0$ , using the thermodynamic expression [39]:

$$\frac{N_0}{N_T} = \left[ 1 - \left( \frac{T}{T_c^0} \right)^3 \right] - \frac{3\omega_{\text{arith}}\zeta(2)}{2\omega_{\text{geo}}[\zeta(3)]^{2/3}} \left( \frac{T}{T_c^0} \right)^2 N_T^{-1/3}, \quad (\text{G4})$$

where  $\omega_{\text{arith}} = (\omega_x + \omega_y + \omega_z)/3$  is the arithmetic mean of the trapping frequencies, and  $T_c^0 = 177$  nK is the ideal gas critical temperature for the parameters in Ref. [41]. The first term in this equation is simply the ideal-gas relation, and the second accounts for the first-order shift in the critical temperature due to the finite-size of the trapped gas. From  $N_0$ , the chemical potential can then be estimated in the Thomas-Fermi approximation [39]:

$$\mu = \frac{\hbar\omega_{\text{geo}}}{2} \left( \frac{15N_0a_s}{l_{\text{geo}}} \right)^{2/5}. \quad (\text{G5})$$

This value of  $\mu$  is then used to set the energy cutoff  $\epsilon_{\text{cut}} = 2\mu$  and compute the 2D background density as described above.

- 
- [1] W. H. Zurek, U. Dörner, and P. Zoller, Dynamics of a Quantum Phase Transition, *Phys. Rev. Lett.* **95**, 105701 (2005).
- [2] J. M. Kosterlitz and D. J. Thouless, Ordering, metastability and phase transitions in two-dimensional systems, *J. Phys. C* **6**, 1181 (1973).
- [3] V. L. Berezinskii, Destruction of long-range order in one-dimensional and two-dimensional systems possessing a continuous symmetry group. II. Quantum systems, *Sov. J. Exp. Theor. Phys.* **34**, 610 (1972).
- [4] A. C. Mathey, C. W. Clark, and L. Mathey, Decay of a superfluid current of ultracold atoms in a toroidal trap, *Phys. Rev. A* **90**, 023604 (2014).
- [5] S. J. Rooney, T. W. Neely, B. P. Anderson, and A. S. Bradley, Persistent-current formation in a high-temperature Bose-Einstein condensate: An experimental test for classical-field theory, *Phys. Rev. A* **88**, 063620 (2013).
- [6] A. A. Abrikosov, The magnetic properties of superconducting alloys, *J. Phys. Chem. Solids* **2**, 199 (1957).
- [7] A. L. Fetter, Vortices in an imperfect Bose gas. IV. Translational velocity, *Phys. Rev.* **151**, 100 (1966).
- [8] V. Ambegaokar, B. I. Halperin, D. R. Nelson, and E. D. Siggia, Dynamics of superfluid films, *Phys. Rev. B* **21**, 1806 (1980).
- [9] G. Gauthier, M. T. Reeves, X. Yu, A. S. Bradley, M. A. Baker, T. A. Bell, H. Rubinsztein-Dunlop, M. J. Davis, and T. W. Neely, Giant vortex clusters in a two-dimensional quantum fluid, *Science* **364**, 1264 (2019).
- [10] S. P. Johnstone, A. J. Groszek, P. T. Starkey, C. J. Billington, T. P. Simula, and K. Helmersson, Evolution of large-scale flow from turbulence in a two-dimensional superfluid, *Science* **364**, 1267 (2019).
- [11] O. R. Stockdale, M. T. Reeves, X. Yu, G. Gauthier, K. Goddard-Lee, W. P. Bowen, T. W. Neely, and M. J. Davis, Universal dynamics in the expansion of vortex clusters in a dissipative two-dimensional superfluid, *Phys. Rev. Res.* **2**, 033138 (2020).
- [12] M. T. Reeves, K. Goddard-Lee, G. Gauthier, O. R. Stockdale, H. Salman, T. Edmonds, X. Yu, A. S. Bradley, M. Baker, H. Rubinsztein-Dunlop *et al.*, Turbulent Relaxation to Equilibrium in a Two-Dimensional Quantum Vortex Gas, *Phys. Rev. X* **12**, 011031 (2022).
- [13] L. Onsager, Statistical hydrodynamics, *Nuovo Cimento* **6**, 279 (1949).
- [14] T. P. Billam, M. T. Reeves, and A. S. Bradley, Spectral energy transport in two-dimensional quantum vortex dynamics, *Phys. Rev. A* **91**, 023615 (2015).
- [15] M. T. Reeves, T. P. Billam, B. P. Anderson, and A. S. Bradley, Inverse Energy Cascade in Forced Two-Dimensional Quantum Turbulence, *Phys. Rev. Lett.* **110**, 104501 (2013).
- [16] T. P. Billam, M. T. Reeves, B. P. Anderson, and A. S. Bradley, Onsager-Kraichnan Condensation in Decaying Two-Dimensional Quantum Turbulence, *Phys. Rev. Lett.* **112**, 145301 (2014).
- [17] J. H. Kim, W. J. Kwon, and Y. Shin, Role of thermal friction in relaxation of turbulent Bose-Einstein condensates, *Phys. Rev. A* **94**, 033612 (2016).
- [18] W. J. Kwon, G. Moon, J.-Y. Choi, S. W. Seo, and Y.-I. Shin, Relaxation of superfluid turbulence in highly oblate Bose-Einstein condensates, *Phys. Rev. A* **90**, 063627 (2014).
- [19] H. E. Hall, W. F. Vinen, and D. Shoenberg, The rotation of liquid helium II. The theory of mutual friction in uniformly rotating helium II, *Proc. R. Soc. London A* **238**, 215 (1956).
- [20] S. V. Iordanskii, Mutual friction force in a rotating Bose gas, *J. Exp. Theor. Phys.* **22**, 160 (1966).
- [21] C. F. Barenghi, R. J. Donnelly, and W. F. Vinen, Friction on quantized vortices in helium II. A review, *J. Low Temp. Phys.* **52**, 189 (1983).
- [22] H. Helmholtz, LXIII. On Integrals of the hydrodynamical equations, which express vortex-motion, *Lond. Edinb. Dublin Philos. Mag. J. Sci.* **33**, 485 (1867).
- [23] G. R. Kirchhoff, *Vorlesungenüber Mathematische Physik: Mechanik* (B.G. Teubner, Leipzig, 1876), Vol. 1.
- [24] P. B. Blakie, A. S. Bradley, M. J. Davis, R. J. Ballagh, and C. W. Gardiner, Dynamics and statistical mechanics of ultracold Bose gases using c-field techniques, *Adv. Phys.* **57**, 363 (2008).
- [25] N. P. Proukakis and B. Jackson, Finite-temperature models of Bose-Einstein condensation, *J. Phys. B: At. Mol. Opt. Phys.* **41**, 203002 (2008).
- [26] G. Moon, W. J. Kwon, H. Lee, and Y.-I. Shin, Thermal friction on quantum vortices in a Bose-Einstein condensate, *Phys. Rev. A* **92**, 051601(R) (2015).
- [27] W. J. Kwon, G. Del Pace, K. Khani, L. Galantucci, A. Muzi Falconi, M. Inguscio, F. Scazza, and G. Roati, Sound emission

- and annihilations in a programmable quantum vortex collider, *Nature (London)* **600**, 64 (2021).
- [28] O. Törnkvist and E. Schröder, Vortex Dynamics in Dissipative Systems, *Phys. Rev. Lett.* **78**, 1908 (1997).
- [29] A. S. Bradley, C. W. Gardiner, and M. J. Davis, Bose-Einstein condensation from a rotating thermal cloud: Vortex nucleation and lattice formation, *Phys. Rev. A* **77**, 033616 (2008).
- [30] S. J. Rooney, P. B. Blakie, and A. S. Bradley, Numerical method for the stochastic projected Gross-Pitaevskii equation, *Phys. Rev. E* **89**, 013302 (2014).
- [31] S. J. Rooney, A. J. Allen, U. Zülicke, N. P. Proukakis, and A. S. Bradley, Reservoir interactions of a vortex in a trapped three-dimensional Bose-Einstein condensate, *Phys. Rev. A* **93**, 063603 (2016).
- [32] A. S. Bradley and P. B. Blakie, Stochastic projected Gross-Pitaevskii equation for spinor and multicomponent condensates, *Phys. Rev. A* **90**, 023631 (2014).
- [33] A. S. Bradley, S. J. Rooney, and R. G. McDonald, Low-dimensional stochastic projected Gross-Pitaevskii equation, *Phys. Rev. A* **92**, 033631 (2015).
- [34] Z. Mehdi, A. S. Bradley, J. J. Hope, and S. S. Szigeti, Superflow decay in a toroidal Bose gas: The effect of quantum and thermal fluctuations, *SciPost Phys.* **11**, 080 (2021).
- [35] Although we neglect an explicit projector onto the low-energy subspace, since it does not significantly affect systems with homogeneous density, such projection is still implicitly included through the energy-cutoff dependence of the scattering kernel.
- [36] In general, the effective scattering potential takes the form  $V_{\varepsilon} = -\hbar \int d^2\mathbf{r}' \varepsilon(\mathbf{r} - \mathbf{r}') \nabla' \cdot \mathbf{j}'$ , where  $\mathbf{j}$  is the particle current [24]. To obtain Eq. (3), we have employed the continuity equation  $\nabla \cdot \mathbf{j} + \partial_t \rho = 0$ , which holds exactly for Eq. (2), but is weakly violated by the number-damping reservoir process; leading order corrections are  $O(\gamma) \ll 1$ .
- [37] A. Lucas and P. Surówka, Sound-induced vortex interactions in a zero-temperature two-dimensional superfluid, *Phys. Rev. A* **90**, 053617 (2014).
- [38] This expression has an additional factor of two compared to that of Ref. [37], which is required for agreement between the conserved energy of the above Lagrangian and the GPE Hamiltonian. We have numerically confirmed this for the case of a well-separated vortex dipole.
- [39] F. Dalfó, S. Giorgini, L. P. Pitaevskii, and S. Stringari, Theory of Bose-Einstein condensation in trapped gases, *Rev. Mod. Phys.* **71**, 463 (1999).
- [40] C. J. Pethick and H. Smith, *Bose-Einstein Condensation in Dilute Gases* (Cambridge University Press, Cambridge, 2008).
- [41] B. Jackson, N. P. Proukakis, C. F. Barenghi, and E. Zaremba, Finite-temperature vortex dynamics in Bose-Einstein condensates, *Phys. Rev. A* **79**, 053615 (2009).
- [42] S. J. Rooney, P. B. Blakie, B. P. Anderson, and A. S. Bradley, Suppression of Kelvin-induced decay of quantized vortices in oblate Bose-Einstein condensates, *Phys. Rev. A* **84**, 023637 (2011).
- [43] W. F. Vinen, Mutual friction in a heat current in liquid helium II. III. Theory of the mutual friction, *Proc. R. Soc. London A* **242**, 493 (1957).
- [44] P. O. Fedichev and G. V. Shlyapnikov, Dissipative dynamics of a vortex state in a trapped Bose-condensed gas, *Phys. Rev. A* **60**, R1779 (1999).
- [45] Corrections due to weak density gradients could be included under a local density approximation, giving spatially dependent damping and diffusion coefficients based on local density at each vortex, e.g.,  $\alpha(\mathbf{r}_n) \propto \rho_0(\mathbf{r}_n)$ .
- [46] Agreement is significantly better for the lower temperature points, where the thermal density does not vary as strongly.
- [47] A. Groszek, M. Davis, and T. Simula, Decaying quantum turbulence in a two-dimensional Bose-Einstein condensate at finite temperature, *SciPost Phys.* **8**, 039 (2020).
- [48] P. W. Adams and W. I. Glaberson, Vortex dynamics in superfluid helium films, *Phys. Rev. B* **35**, 4633 (1987).
- [49] K. A. Gillis, S. M. Volz, and J. M. Mochel, Velocity-dependent dissipation from free vortices and bound vortex pairs below the Kosterlitz-Thouless transition, *Phys. Rev. B* **40**, 6684 (1989).
- [50] Z. Wu, S. Zhang, and H. Zhai, Dynamic Kosterlitz-Thouless theory for two-dimensional ultracold atomic gases, *Phys. Rev. A* **102**, 043311 (2020).
- [51] N. Prokof'ev, O. Ruebenacker, and B. Svistunov, Critical Point of a Weakly Interacting Two-Dimensional Bose Gas, *Phys. Rev. Lett.* **87**, 270402 (2001).
- [52] J. L. Ville, R. Saint-Jalm, É. Le Cerf, M. Aidelsburger, S. Nascimbène, J. Dalibard, and J. Beugnon, Sound Propagation in a Uniform Superfluid Two-Dimensional Bose Gas, *Phys. Rev. Lett.* **121**, 145301 (2018).
- [53] R. G. McDonald and A. S. Bradley, Brownian motion of a matter-wave bright soliton moving through a thermal cloud of distinct atoms, *Phys. Rev. A* **93**, 063604 (2016).
- [54] R. G. McDonald, P. S. Barnett, F. Atayee, and A. Bradley, Dynamics of hot Bose-Einstein condensates: Stochastic Ehrenfest relations for number and energy damping, *SciPost Phys.* **8**, 029 (2020).
- [55] S. Nazarenko and M. Onorato, Wave turbulence and vortices in Bose-Einstein condensation, *Physica D* **219**, 1 (2006).
- [56] M. Gałka, P. Christodoulou, M. Gazo, A. Karailiev, N. Dogra, J. Schmitt, and Z. Hadzibabic, Emergence of Isotropy and Dynamic Scaling in 2D Wave Turbulence in a Homogeneous Bose Gas, *Phys. Rev. Lett.* **129** (2022).
- [57] A. S. Bradley and B. P. Anderson, Energy Spectra of Vortex Distributions in Two-Dimensional Quantum Turbulence, *Phys. Rev. X* **2**, 041001 (2012).
- [58] S. J. Rooney, A. S. Bradley, and P. B. Blakie, Decay of a quantum vortex: Test of nonequilibrium theories for warm Bose-Einstein condensates, *Phys. Rev. A* **81**, 023630 (2010).